Mass Spectrometry Imaging Reveals Molecular Changes Associated with Aging in Pancreatic Cancer

Erin H. Seeley[1], Jimin Min[2], Jared K. Burks[2], Paola A. Guerrero[2], Anirban Maitra[2]
[1]The University of Texas at Austin, Austin, TX, [2]UT MD Anderson Cancer Center, Houston, TX

Overview

- Spatial omics provides important molecular localization information that is lost with bulk omics analyses
- Careful sample preparation allowed for sequential mass spectrometry imaging (MSI) of metabolites, N-linked glycans, and tryptic peptides from the same tissue section followed by histological staining
- MSI data can be integrated with other spatial omics data to achieve a deeper understanding of molecular changes with aging in PDAC

Introduction

Aging is one of the most important risk factors for pancreatic ductal adenocarcinoma (PDAC) with the typical median age of onset in the 70s at the time of diagnosis. However, a subset of patients experiences disease onset much earlier, especially among women, without any known genetic predisposition. The increasing recognition of age-associated pancreatic cancer incidence necessitates understanding diverse molecular changes associated with variations in age of onset and gender. Mass spectrometry imaging allows for detection of hundreds of biomolecules from tissue sections without target-specific reagents and multiple classes of analytes can be analyzed from the same section using sequential imaging. Here, we seek to interrogate molecular differences between early and typical onset pancreatic cancer as well as any gender-specific differences.

Methods

FFPE tissue sections were dewaxed with xylene before being coated with DAN matrix using an HTX M5 Robotic Sprayer. Metabolite images were collected in negative ion mode using a Bruker timsTOF fleX MALDI QTOF mass spectrometer. After image collection, matrix was removed and PNGase F digestion was performed on the same section before coating with CHCA matrix and N-glycan image collection. Subsequent to N-glycan imaging, matrix was removed and tryptic digestion was performed on the same section before coating with CHCA and peptide image collection. All images were collected at 20 µm resolution. Finally, the imaged sections were H&E stained for histological evaluation. Image visualization was performed using SCiLS Lab Pro and metabolite and glycan identification were carried out using MetaboScape.

Workflow

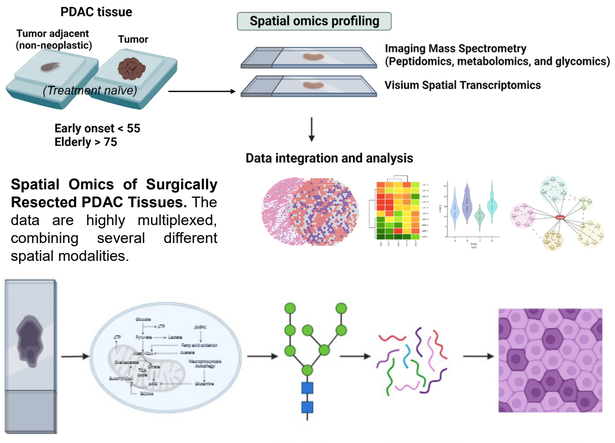

Spatial Omics of Surgically Resected PDAC Tissues. The data are highly multiplexed, combining several different spatial modalities.

Mass Spectrometry Imaging Workflow. All 3 datasets are acquired sequentially from the same tissue section, allowing for direct registration of the data. *Created with BioRender.com*

Patient Demographics

ID	Tissue type	Gender	Age	pT	pN	Group_age	Group_gender
EOPC-1	PDAC	M	39.8	2	2	Younger	Male
EOPC-2	PDAC	F	49.1	2	2	Younger	Female
UOPC-1	PDAC	M	81.4	2	0	Older	Male
UOPC-2	PDAC	F	77.1	3	1	Older	Female
EOPC-3	PDAC	M	24.9	3	2	Younger	Male
EOPC-4	PDAC	F	52.3	2	1	Younger	Female
UOPC-3	PDAC	M	79.9	2	2	Older	Male
UOPC-4	PDAC	F	80.9	2	1	Older	Female
EOPC-5	PDAC	M	49.8	2	2	Younger	Male
EOPC-6	PDAC	F	51.3	3	2	Younger	Female
UOPC-5	PDAC	M	77.3	2	0	Older	Male
UOPC-6	PDAC	F	78.9	1	2	Older	Female
EOPC-7	PDAC	F	53.8	2	1	Younger	Female
EOPC-8	PDAC	M	54.7	2	2	Younger	Male
UOPC-7	PDAC	F	84.8	2	2	Older	Female
UOPC-8	PDAC	M	78.2	3	2	Older	Male

Mass Spectrometry Imaging

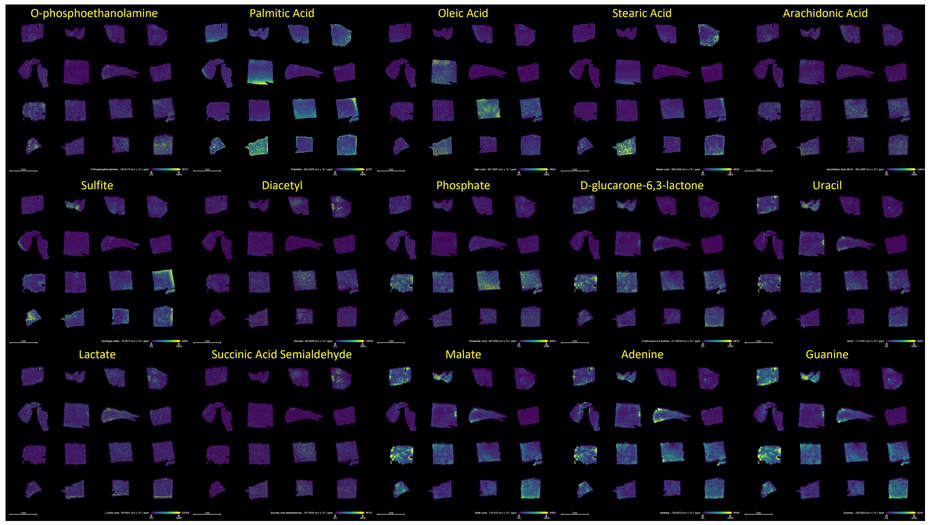

Spatial Metabolomic Imaging of PDAC Samples. Numerous small metabolites were detected in PDAC samples. The top row shows molecules involved in fatty acid metabolism. Interestingly, different fatty acid show different spatial distributions. The saturated fatty acids (palmitic and stearic acid) show similar distributions while the unsaturated fatty acids (oleic and arachidonic acid) show similar patterns to each other, but different from the saturated fatty acids. The middle and bottom rows display inorganic nutrients, TCA cycle molecules, nucleobases, and energy metabolites. Malate and guanine appear to be slightly more abundant in the samples from early onset patients (left two columns in each image) while succinic acid semialdehyde is more abundant in the elderly patients (right two columns in each image). No gender differences were readily observed in these images. Putative metabolite identifications were generated using MetaboScape. Sample layout is shown in the Histology panel to the right.

Spatial Glycomic Imaging of PDAC Samples. N-linked glycans were released *in situ* by treating the sections with PNGaseF after the metabolite data had been collected. Hundreds of N-glycans were detected in PDAC samples. The top row of images show examples of high mannose glycans, all showing quite similar localization, with higher abundance in the female samples (second and fourth columns in each image). The middle row of images shows examples of hybrid glycans, which display move variability in distributions compared to the high mannose glycans. The bottom row of images shows examples of complex glycans, which also show a considerable variability in their spatial localization. Putative glycan identifications were generated using MetaboScape. Cartoons are only examples of possible N-glycan structures, linkages and exact branch positions have not been determined. Sample layout is shown in the Histology panel to the right.

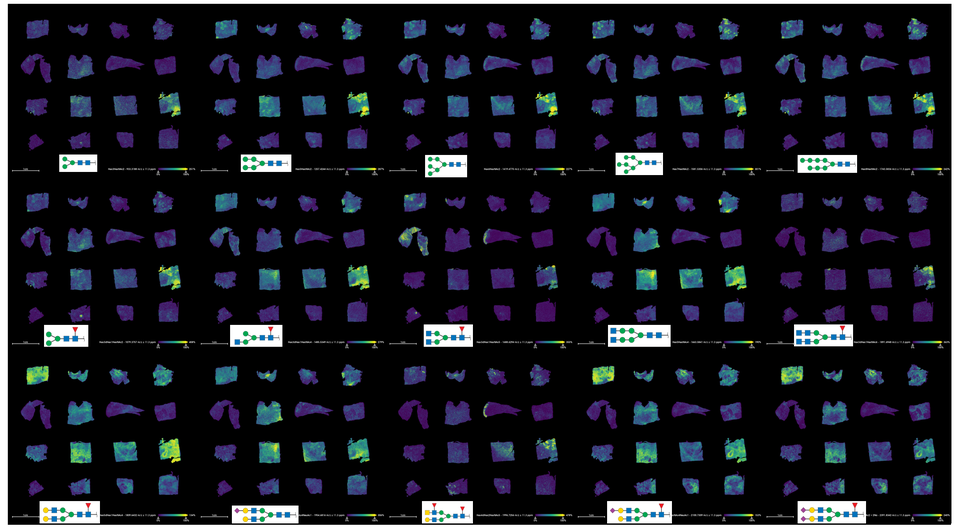

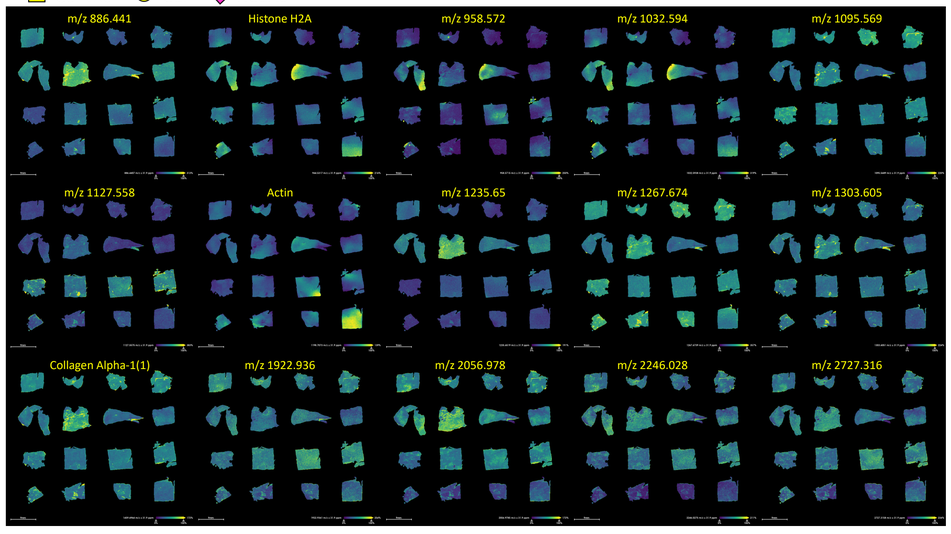

Spatial Peptidomic Imaging of PDAC Samples. Tryptic peptides were generated *in situ* by treating the sections with trypsin after N-linked glycan data had been collected. Hundreds of peptides were detected in PDAC samples. A few putative IDs are included based on work in other MSI studies. For example, Histone H2A is most abundantly observed in areas of high cell density. Collagen is detected in areas of vessels or other connective tissue. Actin appears to be more abundant in the PDAC samples from the elderly patients (right 2 columns of each image). However, in most cases, only a measured *m/z* value is currently known. Ions at *m/z* 958.572 and 1032.594 show similar localization to Histone H2A, which highest abundance in areas of high cell density. Follow up work with LC-MS/MS will enable identification of these currently unnamed peptides. Additionally, correlation with cell segmentation will provide further insight into the observed spatial patterns. Sample layout is shown in the Histology panel to the right.

Co-Registration

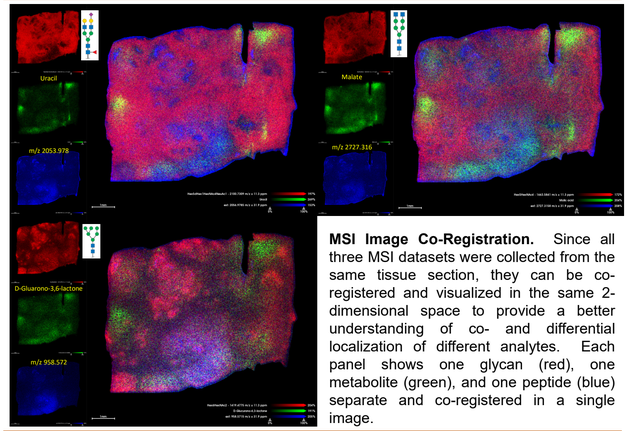

MSI Image Co-Registration. Since all three MSI datasets were collected from the same tissue section, they can be co-registered and visualized in the same 2-dimensional space to provide a better understanding of co- and differential localization of different analytes. Each panel shows one glycan (red), one metabolite (green), and one peptide (blue) separate and co-registered in a single image.

Histology

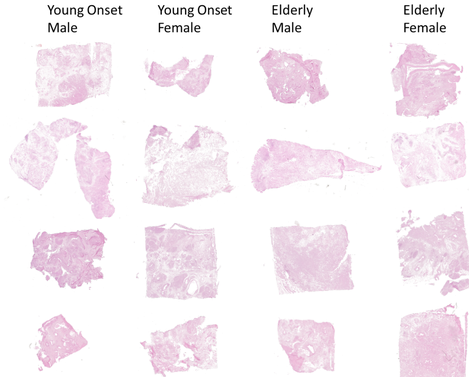

After all three MS images had been collected, the MALDI matrix was removed and the sections were H&E stained. The layout shown here is the same for all MSI data.

Spatial Transcriptomics

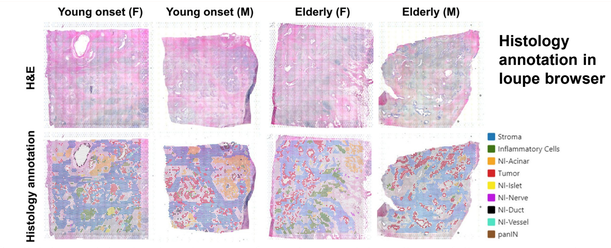

Spatial transcriptomics has been performed on serial sections of the same samples. Tissue segmentation from these analyses will be integrated with the MSI spatial omics data to obtain a deeper understanding of the role of aging in pancreatic cancer.

Conclusions

- Three separate mass spectrometry imaging experiments could be carried out on the same tissue section with no loss of data quality
- Localization differences were observed via mass spectrometry imaging with respect to cell type, age, and gender, information that would be lost in bulk analyses
- The addition of tissue segmentation and integration with other omics data will further our understanding of molecular changes associated with aging in pancreatic ductal adenocarcinoma

Acknowledgements

CPRIT RP190617 RP220610
NIH NATIONAL CANCER INSTITUTE TBEL U54CA274371 1 R50 CA243707-01A1
The Sheikh Khalifa Bin Zayed Al-Nahyan Foundation